DOI: 10.1021/ic902480n

Inorganic Chemistry
Article

How are Centrosymmetric and Noncentrosymmetric Structures Achieved in Uranyl Borates?

Shuao Wang,[†] Evgeny V. Alekseev,*[,‡,†] Jared T. Stritzinger,[†] Wulf Depmeier,[‡] and Thomas E. Albrecht-Schmitt*[,†]

[†]*Department of Civil Engineering and Geological Sciences and Department of Chemistry and Biochemistry, 156 Fitzpatrick Hall, University of Notre Dame, Notre Dame, Indiana 46556, and*
[‡]*Institut für Geowissenschaften, Universität zu Kiel, 24118 Kiel, Germany*

Received December 14, 2009

Four uranyl borates, $UO_2B_2O_4$ (**UBO-1**), α-$(UO_2)_2[B_9O_{14}(OH)_4]$ (**UBO-2**), β-$(UO_2)_2[B_9O_{14}(OH)_4]$ (**UBO-3**), and $(UO_2)_2[B_{13}O_{20}(OH)_3]\cdot 1.25H_2O$ (**UBO-4**), have been prepared from boric acid fluxes at 190 °C. **UBO-3** and **UBO-4** are centrosymmetric, whereas **UBO-1** and **UBO-2** are noncentrosymmetric (chiral and polar). These uranyl borates possess layered structures constructed from UO_8 hexagonal bipyramids, BO_3 triangles, and BO_4 tetrahedra. In the case of **UBO-4**, clusters of BO_3 triangles link the layers together to form open slabs with a thickness of almost 2 nm. The ability of uranyl borates to use very similar layers to yield both centrosymmetric and noncentrosymmetric layers is detailed in this work.

Introduction

Uranyl borates represent a fascinating group of zero-, two-, and three-dimensional materials. A variety of synthetic methods have been employed to prepare these compounds, and the conditions under which these solids form leads to their subdivision into three categories. The first group is a series of chiefly centrosymmetric borates that are primarily constructed from UO_6 tetragonal bipyramids and/or UO_7 pentagonal bipyramids and BO_3 triangles.[1−6] These compounds are derived from high-temperature B_2O_3 melts. The second category has only a single representative, $K_6[UO_2\{B_{16}O_{24}(OH)_8\}]\cdot 12H_2O$, and this compound consists of isolated clusters composed of a cyclic polyborate surrounding a uranyl core.[7] It forms via the slow evaporation of aqueous solutions contain UO_2^{2+} and borate at room temperature. The third group is prepared via the use of boric acid fluxes at relatively low temperatures (ca. 200 °C). These compounds blend features found in both previous categories in that they contain polyborate layers and frameworks that are built from both triangular BO_3 and tetrahedral BO_4 units that surround uranyl cations.[8,9] All of these compounds contain UO_8 hexagonal bipyramids.

As a general class of compounds, borates are known from their applications in optics, especially for their large nonlinear optical responses in the deep UV, where they are much more transparent than most oxoanion compounds.[10−12] In order for a compound to display a second-order nonlinear optical (NLO) response, it must lack a center of symmetry. While borates are known for achieving this, a survey of the space groups of borates reveals that noncentrosymmetric structures are not common, making the preparation of new borate NLO materials challenging.[13,14] We have recently demonstrated that both sodium and thallium uranyl borates are either chiral or polar. Eight such compounds have been reported by us.[8,9] These results are surprising because the presence of the uranyl cation has a propensity for yielding centrosymmetric structures because of the highly symmetric nature of UO_2^{2+}. Nevertheless, all of the uranyl borates that we have prepared that contain additional monovalent cations are noncentrosymmetric.[9] However, we know that centrosymmetric structures are possible in actinyl borates from the structures of the neptunyl borates, $K_4(NpO_2)_{6.73}B_{20}O_{36}(OH)_2$ and $Ba_2(NpO_2)_{6.59}B_{20}O_{36}(OH)_2\cdot H_2O$.[8]

*To whom correspondence should be addressed. E-mail: talbrec1@nd.edu.

(1) Gasperin, M. *Acta Crystallogr.* **1987**, *C43*, 1247.
(2) Gasperin, M. *Acta Crystallogr.* **1987**, *C43*, 2031.
(3) Gasperin, M. *Acta Crystallogr.* **1987**, *C43*, 2264.
(4) Gasperin, M. *Acta Crystallogr.* **1988**, *C44*, 415.
(5) Gasperin, M. *Acta Crystallogr.* **1989**, *C45*, 981.
(6) Gasperin, M. *Acta Crystallogr.* **1990**, *C46*, 372.
(7) Behm, H. *Acta Crystallogr., Sect. C* **1985**, *41*, 642.
(8) Wang, S.; Alekseev, E. V.; Ling, J.; Skanthakumar, S.; Soderholm, L.; Depmeier, W.; Albrecht-Schmitt, T. E. *Angew. Chem., Int. Ed.* **2010**, *49*, 1263.
(9) Wang, S.; Alekseev, E. V.; Ling, J.; Liu, G.; Depmeier, W.; Albrecht-Schmitt, T. E. *Chem. Mater.* **2010**, [Online].
(10) Mori, Y.; Yap, Y. K.; Kamimura, T.; Yoshimura, M.; Sasaki, T. *Opt. Mater.* **2002**, *19*, 1.
(11) Chen, C.; Wu, B.; Jiang, A.; You, G. *Sci. Sin.* **1984**, *B7*, 598.
(12) Mori, Y.; Sasaki, T. *Bull. Mater. Sci.* **1999**, *22*, 399.
(13) Burns, P. C.; Grice, J. D.; Hawthorne, F. C. *Can. Mineral.* **1995**, *33*, 1131.
(14) Burns, P. C.; Grice, J. D.; Hawthorne, F. C. *Can. Mineral.* **1999**, *37*, 731.

Published on Web 02/16/2010

Table 1. Crystallographic Data for $UO_2B_2O_4$ (**UBO-1**), α-$(UO_2)_2[B_9O_{14}(OH)_4]$ (**UBO-2**), β-$(UO_2)_2[B_9O_{14}(OH)_4]$ (**UBO-3**), and $(UO_2)_2[B_{13}O_{20}(OH)_3]\cdot 1.25H_2O$ (**UBO-4**)

compound	UBO-1	UBO-2	UBO-3	UBO-4
mass	355.65	925.35	925.35	1068.59
color and habit	yellow, block	yellow-green, plate	yellow-green, block	yellow, needle
space group	$C2$	$P2_1$	$P\bar{1}$	$P\bar{1}$
a (Å)	10.4607(9)	6.4534(4)	6.4169(5)	6.4732(5)
b (Å)	4.1863(4)	21.2535(12)	6.4494(5)	10.7981(8)
c (Å)	5.6251(5)	6.4548(4)	11.0177(12)	19.6653(15)
α (deg)	90	90	97.604(1)	85.711(1)
β (deg)	109.769(1)	119.874(1)	92.365(1)	82.660(1)
γ (deg)	90	90	119.475(1)	89.287(1)
V (Å^3)	231.81(4)	767.68(8)	390.46(6)	1359.48(18)
Z	2	2	1	1
T (K)	293(2)	100(2)	296(2)	293(2)
λ (Å)	0.71073	0.71073	0.71073	0.71073
maximum 2θ	28.68	28.83	28.62	28.67
ρ calcd (g cm^{-3})	5.095	4.003	3.935	2.610
μ (Mo Kα)	349.49	212.00	208.41	120.05
$R(F)$ for $F_o^2 > 2\sigma(F_o^2)^a$	0.0139	0.0316	0.0200	0.0558
$Rw(F_o^2)^b$	0.0332	0.0725	0.0447	0.1370

^{a} $R(F) = \sum||F_o| - |F_c||/\sum|F_o|$. ^{b} $R(F_o^2) = [\sum w(F_o^2 - F_c^2)^2/\sum w(F_o^4)]^{1/2}$.

We have recently prepared pure uranyl borates from boric acid fluxes that lack additional cations. Two of these compounds are centrosymmetric; two are noncentrosymmetric. These compounds are $UO_2B_2O_4$ (**UBO-1**), α-$(UO_2)_2[B_9O_{14}(OH)_4]$ (**UBO-2**), β-$(UO_2)_2[B_9O_{14}(OH)_4]$ (**UBO-3**), and $(UO_2)_2[B_{13}O_{20}(OH)_3]\cdot 1.25H_2O$ (**UBO-4**). These uranyl borates are all new, and possess fascinating structures and more importantly provide us with an opportunity to explore how uranyl borates can use similar structural motifs to yield both centrosymmetric and noncentrosymmtric structures, which is the purpose of this article.

Experimental Section

Syntheses. $UO_2(NO_3)_2\cdot 6H_2O$ (98%, International Bio-Analytical Industries), boric acid (99.99%, Alfa-Aesar), ammonium chloride (99.6%, Fisher), and cesium nitrate (99.8%, Alfa-Aesar) were used as received. All the reactions were run in PTFE-lined Parr 4749 autoclaves with a 23 mL internal volume. Distilled and Millipore filtered water with resistance of 18.2 MΩ·cm was used in all reactions. ***Caution!*** *While the* $UO_2(NO_3)_2\cdot 6H_2O$ *used in this study contained depleted U, there is really not much difference between depleted uranium and natural abundance uranium, and standard precautions for handling radioactive materials should be followed at all times. There are very old sources of uranyl nitrate that may not be depleted, and enhanced care is warranted for these samples.*

$UO_2B_2O_4$ (UBO-1). $UO_2(NO_3)_2\cdot 6H_2O$ (0.5000 g, 1 mmol), boric acid (0.4944 g, 8 mmol), and water (50 μL) were loaded into a 23 mL autoclave. The autoclave was sealed and heated to 190 °C in a box furnace for 3 days. The autoclave was then cooled down to room temperature at a rate of 5 °C/h. The products were washed with boiling water to remove excess boric acid, followed by rinsing with methanol. Crystals in the form of needles and prisms with light yellow coloration were collected as a pure phase for $UO_2B_2O_4$ (**UBO-1**). Yield: 123 mg (35% based on uranium).

α-$(UO_2)_2[B_9O_{14}(OH)_4]$ and β-$(UO_2)_2[B_9O_{14}(OH)_4]$ (UBO-2 and UBO-3). $UO_2(NO_3)_2\cdot 6H_2O$ (0.5000 g, 1 mmol), boric acid (1.3586 g, 22 mmol), ammonium chloride (0.0535 g, 1 mmol), and water (50 μL) were loaded into a 23 mL autoclave. The autoclave was sealed and heated to 190 °C in a box furnace for 3 days. The autoclave was then cooled down to room temperature at a rate of 5 °C/h. The products were washed with boiling water to remove excess boric acid, followed by rinsing with methanol. Crystals in the form of plates and blocks with light yellow-green coloration were collected for α-$(UO_2)_2[B_9O_{14}(OH)_4]$ and β-$(UO_2)_2[B_9O_{14}(OH)_4]$ (**UBO-2** and **UBO-3**). **UBO-1** is also present as a minor product.

$(UO_2)_2[B_{13}O_{20}(OH)_3]\cdot 1.25H_2O$ (UBO-4). $UO_2(NO_3)_2\cdot 6H_2O$ (0.5000 g, 1 mmol), boric acid (0.4944 g, 8 mmol), cesium nitrate (0.3898 g, 2 mmol), and water (90 μL) were loaded into a 23 mL autoclave. The autoclave was sealed and heated to 190 °C in a box furnace for 3 days. The autoclave was then cooled down to room temperature at a rate of 5 °C/h. The products were washed with boiling water to remove excess boric acid, followed by rinsing with methanol. Crystals in the form of needles with light yellow coloration were collected as a pure phase for $(UO_2)_2[B_{13}O_{20}(OH)_3]\cdot 1.25H_2O$ (**UBO-4**). Yield: 144 mg (27% based on uranium).

Crystallographic Studies. Single crystals of all four **UBO** phases were mounted on glass fibers and optically aligned on a Bruker APEXII CCD X-ray diffractometer or a Bruker APEXII Quazar X-ray diffractometer using a digital camera. Initial intensity measurements were either performed using an IμS X-ray source, a 30 W microfocused sealed tube (Mo Kα, λ = 0.71073 Å) with high-brilliance and high-performance focusing Quazar multilayer optics, or a standard sealed tube with a monocapillary collimator. Standard APEXII software was used for determination of the unit cells and data collection control. The intensities of reflections of a sphere were collected by a combination of four sets of exposures (frames). Each set had a different φ angle for the crystal, and each exposure covered a range of 0.5° in ω. A total of 1464 frames were collected with an exposure time per frame of 10 to 50 s, depending on the crystal. The SAINT software was used for data integration including Lorentz and polarization corrections. Semiempirical absorption corrections were applied using the program SADABS.[15] Selected data and crystallographic information are listed in Table 1. Atomic coordinates, bond distances, and additional structural information are provided in the Supporting Information (CIF).

Powder X-Ray Diffraction. Powder X-ray diffraction patterns of products of pure **UBO-1** and relatively pure **UBO-4** were collected on a Scintag $\theta-\theta$ diffractometer equipped with a diffracted-beamed monochromatic set for Cu Kα (λ = 1.54056 Å) radiation at room temperature in the angular range from 5° to 80° (2θ) with a scanning step width of 0.05° and a fixed counting time of 1 s/step. The collected patterns were

(15) Sheldrick, G. M. SADABS 2001, Program for absorption correction using SMART CCD based on the method of Blessing: Blessing, R. H. *Acta Crystallogr.* **1995**, *A51*, 33.

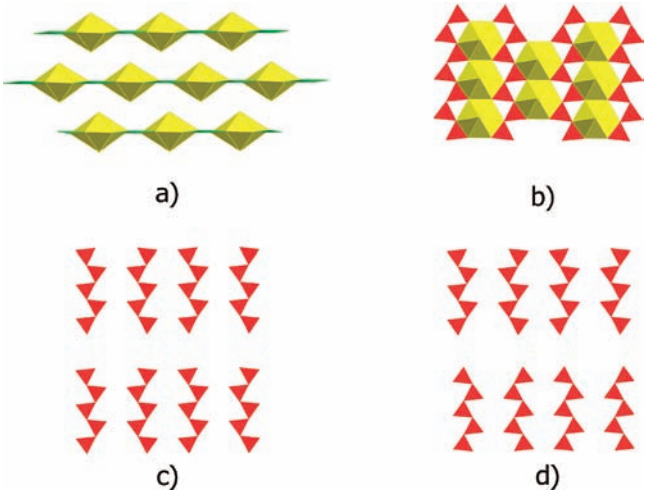

Figure 1. (a) A view of the **UBO-1** crystal structure. (b) The structure of the uranyl borate sheets in **UBO-1**. (c) The relative positions of the layers in α-**UBO-1**. (d) The relative positions of the layers in *β*-**UBO-1**.

compared with those calculated from single crystal data using ATOMS (see the Supporting Information).

Infrared Spectroscopy. Infrared spectra were obtained from a single crystal of **UBO-4** using a SensIR technology IlluminatIR FT-IR microspectrometer. A single crystal of **UBO-4** was placed on a glass slide, and the spectrum was collected with a diamond ATR objective. Each spectrum was taken from 650 to 4000 cm^{-1} with a beam aperture of 100 mm. Infrared spectra are shown in the Supporting Information.

Fluorescence Spectroscopy. Fluorescence data were acquired on all four compounds from single crystals using a Craic Technologies UV−vis−NIR microspectrophotometer with a fluorescence attachment. Excitation was achieved using 365 nm light from a mercury lamp. The fluorescence spectra are provided in the Supporting Information.

Results and Discussion

Synthesis. Boric acid becomes a reactive flux when the reaction temperature is raised above its melting point (170.9 °C). It is an ideal flux for prepared novel actinide borates.[8,9,16] $UO_2B_2O_4$ (**UBO-1**) is observed in reactions that contain high U/B ratios when alkali metal or alkaline-earth metal cations are also present. It can be made as a pure phase when the U/B ratio is higher than 1:8 when additional cations are not present. α-$(UO_2)_2[B_9O_{14}(OH)_4]$ (**UBO-2**) and *β*-$(UO_2)_2[B_9O_{14}(OH)_4]$ (**UBO-3**) form simultaneously in the presence of ammonium chloride. We were surprised to find that NH_4^+ does not directly incorporate into uranyl borates in the same way that alkali metal cations and Tl^+ do.[9] Although its presence plays a definite role in crystallization. Similarly, $(UO_2)_2[B_{13}O_{20}(OH)_3]\cdot 1.25H_2O$ (**UBO-4**) can only be isolated in the presence of trace amounts of Cs^+. In contrast, cesium uranyl borates can be prepared, but these are the subject of a subsequent work. The yields reported in this work are with three day reaction times. We know that yields can be improved with substantially longer heating times (> 7 days).

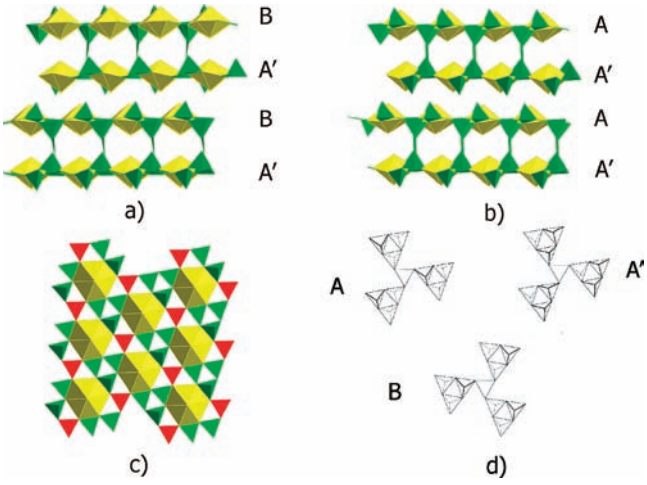

Figure 2. (a) A depiction of the **UBO-2** crystal structure. (b) A general view of the **UBO-3** crystal structure. (c) The structure of borate sheets in **UBO-2** and **UBO-3**. (d) The three topologies of uranyl borate layers realized in **UBO-2** and **UBO-3**.

Structure Descriptions. The structures of all synthesized phases are based on single (**UBO-1**) or double layers (**UBO-2**, **UBO-3**, and **UBO-4**). The simplest sheets are realized in the crystal structure of **UBO-1** (Figure 1). They are based on BO_3 triangles linked by vertices into $(BO_2)_{1\infty}$ 1D zigzag-like chains (Figure 1a). These chains are united into 2D layers by edge-sharing with UO_8 hexagonal bipyramids that also form a 1D chain with a $(UO_6)_{1\infty}$ composition. The resulting layers pack into a regular 3D structure (Figure 1a) with weak connectivity (mostly via van der Waals forces). **UBO-1** is a second modification of a previously known uranyl borate with the $UO_2B_2O_4$ composition.[2] However, this phase was synthesized using a high-temperature solid-state reaction at 1150 °C. The temperature of preparation and symmetry are higher for the modification obtained by Gasperin,[2] and we are referring to this modification as *β*-$UO_2B_2O_4$ in this work. Both modifications are based on identical 2D sheets (Figure 1a), but the orientation of them is different in α-$UO_2B_2O_4$ versus *β*-$UO_2B_2O_4$. In Figure 1c, it is demonstrated that the $(BO_2)_{1\infty}$ chains are arranged in identical positions in sequential layers in α-$UO_2B_2O_4$. However, as shown in Figure 1d, the $(BO_2)_{1\infty}$ chains in *β*-$UO_2B_2O_4$ are arranged differently as the sheets are stacked. The layered structure of *β*-$UO_2B_2O_4$ is identical but oriented differently—the neighboring sheets are rotated by 180° to each other. This rotation is produced by doubling the *c* parameter in *β* modification. This type of polymorphism can be referred to as rotational polytypism as described early on for micas.[17]

The **UBO-2** and **UBO-3** compounds have identical chemical compositions but crystallize in different space groups. We named **UBO-2** as α-$(UO_2)_2[B_9O_{14}(OH)_4]$ and **UBO-3** as the *β* modification. Both phases have layered structures but are very different from **UBO-1** in that they possess double layers that are based on two sublayers (Figure 2a and b). These sublayers consist of 2D polyborate sheets that incorporate the nearly linear uranyl groups, UO_2^{2+}, creating UO_8 hexagonal bipyramids. The borate sheets are based on BO_4 tetrahedra packed in a

(16) Wang, S.; Alekseev, E. V.; Diwu, J.; Casey, W. H.; Phillips, B. L.; Depmeier, W.; Albrecht-Schmitt, T. E. *Angew. Chem., Int. Ed.* **2010**, *49*, 1057.

(17) Takéuchi, Y.; Sadanaga, R. *Acta Crystallogr.* **1959**, *12*, 945.

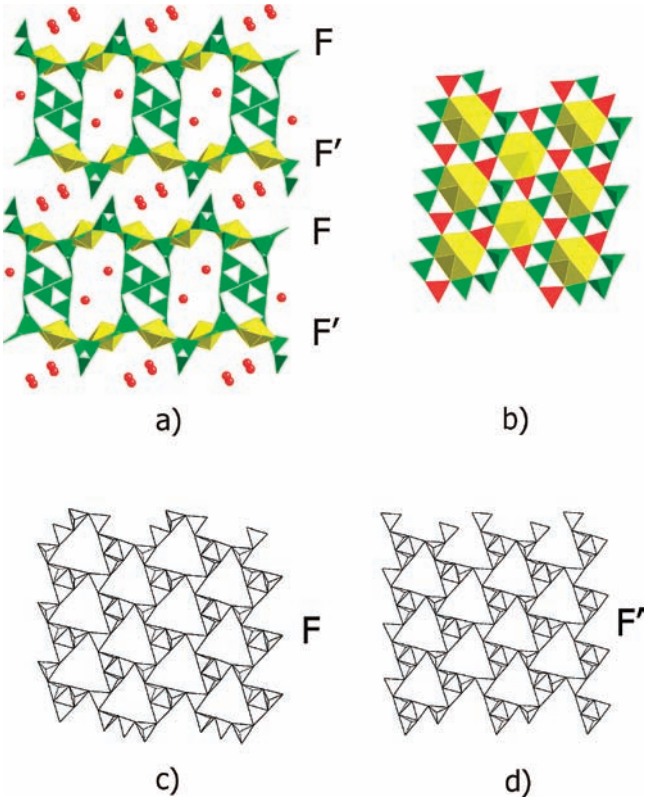

Figure 3. (a) An illustration of the **UBO-4** crystal structure. (b) The structure of uranyl borate sheets in **UBO-4**. (c and d) The two topologies of uranyl borate sheets realized in **UBO-4**.

triangular manner (shown in green color in Figure 2c) and BO_3 triangles (shown in red in Figure 2c), which combine these triangular groups into a 2D network. These 2D sheets are united by perpendicular BO_3 groups into double layers. The resulting layers are packed with a slight shift into a 3D structure. The layers are connected by strong hydrogen bonds with a bond length of 2.42 Å between the O(15) and O(22) oxygen atoms.

The polymorphism in **UBO-2** and **UBO-3** is of a different nature than the polymorphism in $UO_2B_2O_4$. In general, we can follow this in the same way that we used to describe the Na-uranyl borates and Tl-uranyl borates.[9] In this work, we illustrated several different types of borate sheets. In the structures of **UBO-2** and **UBO-3**, three of these sheets, A, A′, and B (Figure 2d), occur. In the α phase, there are alternating enantiomorphic A′ and B layers, and the resulting structure is chiral and polar. In the β phase, only similar A and A′ layers are found, and they create a symmetry center in **UBO-3**.

It is unusual that, in all of the uranyl borate systems (U−B, Na−U−B, and Tl−U−B) that we have prepared, polymorphism is observed. These include α,β-$UO_2B_2O_4$, α,β-$(UO_2)_2[B_9O_{14}(OH)_4]$ (this work), α,β-$Na[(UO_2)_2B_{10}O_{15}(OH)_5)]$, and α,$\beta$-$Tl_2[(UO_2)_2B_{11}O_{18}(OH)_3]$.[9] Such polymorphic richness is very surprising for uranyl chemistry and makes the uranyl borate system unique within groups of binary and ternary uranyl compounds.

The layers in **UBO-4** are also doubled as found in structures of **UBO-2** and **UBO-3** (Figure 3a), but there are substantial differences as well because the layers in **UBO-4** have a nanoscale thickness of ~19 Å. The thick slabs are the result of very unusual linkers and additional

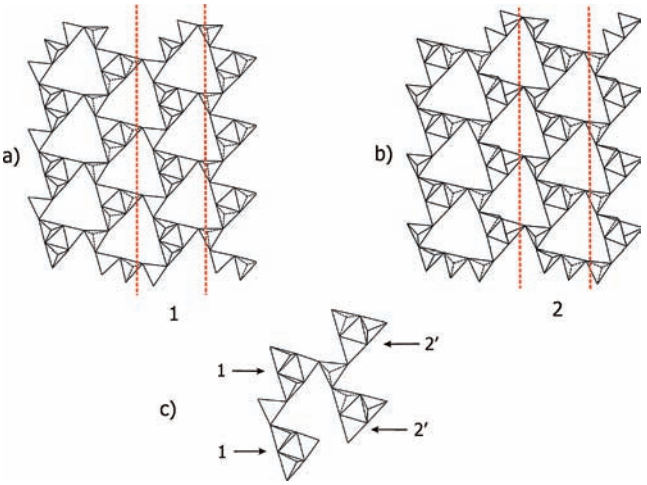

Figure 4. A schematic representation of F-type layer construction using neptunyl and plutonyl borate sheets. (a) Neptunyl borate sheet structure. (b) Plutonyl borate sheet structure. (c) Resulting sheet with F-type topology.

triangular BO_3 groups on both sides (top and bottom) of the layers, as shown in Figure 3a. The linkers in doubled layers consist of one BO_3 group connected with two BO_4 tetrahedra within the sublayers, and a supertriangle that is the second part of the linker. This supertriangle consists of three flat BO_3 groups combined by corners within the supertriangle, and with the BO_4 and BO_3 groups from layers (Figure 3a). These supertriangles are perpendicular to the sublayer planes, and their position produces large free space within the layers that is occupied by disordered water molecules. The sublayers in **UBO-4** are slightly corrugated, and as a result of this, the uranyl groups are not strongly perpendicular to the plane of the layer. The topology of the sublayers is different from all previously known types in actinide borate sheets.[1−9,18] The layers are based on two types of groups that we can call "building blocks" and "linkers." The building blocks consist of two tetrahedral BO_4 groups (directed on one side) and one BO_3 triangle. All of these units share corners, and the projection of it onto the sublayer's plane is triangular-like. The building blocks are united by two sorts of "linkers"; these are BO_3 triangles and BO_4 tetrahedra. These groups are linked together into building blocks that yield a regular 2D network, as shown in Figure 3b, which we call F-type (Figure 3c,d) layers. In the structure of **UBO-4**, there are F type and symmetrically dependent F′ layers (for symmetry details, see ref 9). Both sheets take place in one double layer. The general topology of these sheets is new, but it can be represented as the superposition of the sheets realized in neptunyl and plutonyl borates.[8] The scheme of this construction is shown in Figure 4. In Figure 4a and b, fragments of the sheets in neptunyl and plutonyl borates are shown, respectively. The dashed line shows selected 1D fragments separated from both structures. These are fragments 1 and 2. Fragment 2 can be transformed to 2′ by reflection in the sheet plane (identical to the reverse view). In Figure 4c, it is demonstrated that the results of the 1 and 2′ 1D fragments are combined into the 2D structure where these fragments are regularly alternated. The resulting sheet is

(18) Burns, P. C. *Can. Mineral.* **2005**, *43*, 1839.

identical with F (or F′ after symmetrical transformation). In the same manner, we can create the E-type sheets in uranyl borates that are found in α-$Tl_2[(UO_2)_2B_{11}O_{18}(OH)_3]$. However, the E layer construction found the neptunyl borate sheets are the result of only one BO_4 tetrahedral linker.[8]

The layers in **UBO-4** diverge sharply from other uranyl borates in other ways as well. There are two uranium sites in the layers, both of which are surrounded by nine borate groups. However, one site is surrounded by four BO_3 units and five BO_4 units. The other site is surrounded by three BO_3 units and six BO_4 units, which are also different from the typical uranyl borate coordination environment because these BO_3 units are not separated by two BO_4 units from each other. Interestingly, this coordination environment is exactly the same as the neptunyl borates.[8] The primary difference between **UBO-4** and $K_4(NpO_2)_{6.73}B_{20}O_{36}(OH)_2$ and $Ba_2(NpO_2)_{6.59}B_{20}O_{36}(OH)_2 \cdot H_2O$ is that the neptunyl borates have additional neptunyl units in the voids that are held in place primarily through cation−cation interactions,[8] which are exceedingly rare in U(VI) compounds. The channels that extend within the layers are large at 12.002 × 5.224 Å. In **UBO-4**, the channels are filled with disordered water.

Finally, there is a strong stoichiometric dependence from the reactions that is reflected in the B/U ratio found in the crystals: B/U = 2 (**UBO-1**), B/U = 4.5 (**UBO-2**, **UBO-3**), and B/U = 6.5 (**UBO-4**). The packing principles show only small variations, and in all phases the layers pack to layers, and we observe only 2D structures. However, as the amount of boron is increased, the structures became more 3D-like. **UBO-2** and **UBO-3** (B/U = 4.5) have doubled layers, but very little free space between the layers. However, **UBO-4** (B/U = 6.5) possesses a 3D framework with large voids within and between the layers that are occupied by water molecules. Such structural behavior of the $UO_2^{2+}-B_2O_3$ system is quite unusual because in other similar systems dimensionality decreased with increasing of the X/U ratios (X = Mo, W, P, As, etc.).[19]

Symmetry Features. UBO-1 and **UBO-2** are noncentrosymmetric, whereas **UBO-3** and **UBO-4** possess a center of symmetry. The analysis of the **UBO-1** crystal structure gives a simple understanding of the noncentrosymmetry of this phase. In Figure 1, we can see that the layers alternate and shift. This occurs to maximize close packing. The layers do not have an internal center of symmetry, and the packing type does not produce one as well.

Understanding the lack of a center of symmetry in **UBO-2**, **UBO-3**, and **UBO-4** is more difficult because of the high complexity of these crystal structures. We described the layer types (A/A′, B, and F/F′) in the previous section. The A and B layer types are enantiomorphic (we can name A "right" and B "left", see Figure 2c). Detailed analysis of the **UBO-2** crystal structure demonstrates that the A′ sheets are rotated 30° in comparison to the neighboring B sheets in the plane of the doubled layers (Figure 2a). This rotation is necessary for layers to be linked by the BO_3 triangles, but it makes a center of symmetry impossible within the double layers. The opposite situation occurs in the structure of **UBO-3** (centrosymmetric structure), and there are A and A′ sheets. The A′ sheets are rotated 180° + 1/4*b* shift in comparison with A layers in the same double layers. This rotation is also necessary for the linking of the A and A′ sheets by the BO_3 triangles. This configuration is centrosymmetric because of two equivalent BO_3 linkers (the boron atoms are in split positions). In the structure of **UBO-4**, we can see the same situation. The F and F′ sheets are united in one double layer. The neighboring F sheets also rotated 180° + 1/2*a* + 1/2*b* shift. This is the same situation that occurs in the structure of **UBO-3**, and it also yields a center of symmetry.

A comparison of pure uranyl borates with Na and Tl phases that also possess enantiomorphic sheets yields some interesting results.[9] All eight structures investigated in Na and Tl systems are noncentrosymmetric. Six of them are based on the same sheet alternation as **UBO-2**. The internal rotation of the sheets in these structures is 120°, which is related by 30° in **UBO-2**. There are other structures that are also based on one type of sheet, but centers of symmetry do not occur here because the sheets are rotated by 120° in **NaUBO-4** (as in **UBO-2**) as well as close packing of the same layers (E-type in **TlUBO-1**) in **UBO-1**. Thus, we can say that the achievement of centrosymmetric and noncentrosymmetric structures strongly depends on sheet topologies and the disposition of the sheets as they pack. The relative positions of the sheets are dependent on the chemical compositions. When excess boron is present in the syntheses, doubled layers normally result with additional BO_3 (or B_2O_5 and B_4O_8) groups that link the layers together. As such, we can try to regulate symmetry by adjusting reaction stoichiometry.

Conclusions

Of the 12 uranyl borates that we have now reported, 10 are noncentrosymmetric, the majority of which adopt polar space groups. Of the seven previously reported uranyl borates derived from either B_2O_3 melts or room temperature crystallization, only one is noncentrosymmetric. What makes this result even more surprising is that in some of high-temperature phases the uranium coordination environment is a UO_7 pentagonal bipyramid. This building unit should show a greater propensity for acentric structures than the UO_8 hexagonal bipyramids that we have observed because in the former unit the uranium atoms cannot be placed on centers of inversion (without disorder), whereas in the latter a center of symmetry is easily invoked. Of equal importance is the fact that similar layers that are capable of yielding noncentrosymmetric structures can also yield centrosymmetric structures as found in **UBO-2** and **UBO-3**. In the future, we will disclose other families of uranyl borates that will highlight these themes.

All of these actinide borates provide useful models for the crystallized portions of vitrified nuclear waste.[20−22] These are likely to be one of the only ways that we can glimpse into vitrified nuclear waste because a typical glass log with

(19) Alekseev, E. V.; Krivovichev, S. V.; Armbruster, T.; Depmeier, W.; Suleimanov, E. V.; Chuprunov, E. V.; Golubev, A. V. *Z. Anorg. Allgem. Chem.* **2007**, *633*, 1979.

(20) Ramsey, W. G. *Glass as a Waste Form and Vitrification Technology: Summary of an International Workshop*; National Academy of Science: Washington, 1996.

(21) (a) Krivovichev, S. *Minerals as Advanced Materials I*; Springer: Heidelberg, Germany, 2008. (b) Farnan, I.; Cho, H.; Weber, W. J. *Nature* **2007**, *445*, 190. (c) Ewing, R. C. *Nature* **2007**, *445*, 161. (d) Ewing, R. C. *Proc. Natl Acad. Sci. USA* **1999**, *96*, 3432.

(22) Meaker, T. F. *Neptunium Immobilization and Recovery Using Phase Separated Glasses*; Department of Energy: Washington, DC, 1996.

high-level waste yields on the order of 200,000 Ci (i.e., lethal doses within seconds).

Acknowledgment. We are grateful for support provided by the Chemical Sciences, Geosciences, and Biosciences Division, Office of Basic Energy Sciences, Office of Science, Heavy Elements Program, U.S. Department of Energy, under Grants DE-FG02-01ER15187 and DE-FG02-01ER16026, and by Deutsche Forschungsgemeinschaft for support within the DE 412/30-2 research project. This material is based upon work supported as part of the Materials Science of Actinides, an Energy Frontier Research Center funded by the U.S. Department of Energy, Office of Science, Office of Basic Energy Sciences under Award Number DE-SC0001089. The National Science Foundation also supported a portion of this work through the REU program in solid-state and materials chemistry (DMR).

Supporting Information Available: X-ray crystallographic files in CIF format for $UO_2B_2O_4$ (**UBO-1**), α-$(UO_2)_2[B_9O_{14}(OH)_4]$ (**UBO-2**), β-$(UO_2)_2[B_9O_{14}(OH)_4]$ (**UBO-3**), and $(UO_2)_2[B_{13}O_{20}(OH)_3]\cdot 1.25H_2O$ (**UBO-4**). This material is available free of charge via the Internet at http://pubs.acs.org.